Available online at www.sciencedirect.com
ScienceDirect
Journal of the European Ceramic Society 30 (2010) 2109–2115
www.elsevier.com/locate/jeurceramsoc

Influence of sintering and sintering additives on the mechanical and microstructural characteristics of Si_3N_4/SiC wood cutting tools

C. Strehler [a,*], G. Blugan [a], B. Ehrle [b], B. Speisser [c], T. Graule [a], J. Kuebler [a]

[a] *Empa, Swiss Federal Institute for Materials Testing and Research, Laboratory for High Performance Ceramics, Überlandstrasse 129, CH-8600 Dübendorf, Switzerland*
[b] *OERTLI Werkzeuge AG, Hofstrasse 1, CH-8181 Höri, Switzerland*
[c] *Ceratizit Luxembourg S. à r.l., Route de Holzem, L-8201 Mamer, Luxembourg*

Received 19 October 2009; received in revised form 4 March 2010; accepted 2 April 2010

Abstract

Si_3N_4/SiC cutting tools were fabricated by industrial near net shape fabrication processes. The samples were consolidated by gas-pressure sintering and pressure less sintering using three different additive systems. The mechanical and microstructural properties were compared to composites made by hot pressing. The composites fabricated by gas-pressure sintering showed 99% density, the Vickers hardness was 17.2 GPa and the fracture toughness reached 4.5 $MPa\sqrt{m}$. Machining trials on wood showed that a post-sintering treatment by hot isostatic pressing increases the integrity of the cutting tip due to a devitrification of the intergranular phase.

Keywords: Si_3N_4/SiC composite; Cutting tools; Sintering; Hot isostatic pressing; Mechanical properties

1. Introduction

Industrial wood cutting is a challenging process, as the wood by its nature is inhomogeneous and contains knots, abrasives such as sand and tannins – acids which attack the cutting material. Further, temperatures up to 800 °C can be reached at the cutting tip during wood machining[1] and no coolant can be used as this would impair the surface quality of the cut wood.[2] The lifetime of currently used tungsten carbide (WC) knives is limited by abrasive wear and corrosive attack.[3–5] Si_3N_4 shows superior wear resistance and chemical inertness. It is a hard material with high strength and it can thus withstand high structural loads to high temperatures. SiC has an even higher hardness than Si_3N_4 and additionally a good thermal conductivity.[6] Due to the high hardness, the excellent corrosion resistance, and the lower density compared to hard metals a composite of Si_3N_4 and SiC is a promising material for wood cutting inserts. Because of economical reasons, there is a tendency to increase cutting speed in wood machining.[2] However, the cutting speed (and thus rotation speed) is limited by the centrifugal forces and the clamping forces of the tool holder. Si_3N_4/SiC composites have less than one quarter of the density of WC. Smaller centrifugal forces are therefore acting on the composite knives and the clamping forces can be reduced. This allows the use of lighter tool holders, which enables higher cutting speeds.

In an earlier feasibility study the Si_3N_4/SiC composite showed three times longer lifecycles than commercially available tungsten carbide. Eblagon et al. measured Vickers hardness values of 19.6 GPa and an indentation fracture toughness of 6.7 $MPa\sqrt{m}$.[7] However, the production costs of these composites, which were fabricated by hot pressing followed by diamond cutting, grinding and polishing, were too high for an industrial application. Hence a near net shape processing route involving gas-pressure sintering and hot isostatic pressing has to be followed. Other groups have tried to improve the lifetime of metallic wood cutting tools by covering the knives with anti-abrasive ceramic coatings, such as TiN[8] or CrN.[8,9] Bulk ceramic Al_2O_3-knives have been produced by Gogolewski et al.[10] To our knowledge there are currently no ceramic cutting knives on the market for high speed industrial wood cutting.

Due to the covalent nature of Si_3N_4 and SiC, dense ceramics are produced via liquid phase sintering. The liquid phase is

* Corresponding author.
E-mail address: claudia.strehler@empa.ch (C. Strehler).

0955-2219/$ – see front matter © 2010 Elsevier Ltd. All rights reserved.
doi:10.1016/j.jeurceramsoc.2010.04.007

Table 1
Compositions of the Si_3N_4/SiC ceramics after debinding. The atomic ratio of Al:Y:La was kept constant for all compositions.

	A	B	C
Al_2O_3 [wt%]	1.1	1.6	1.8
Y_2O_3 [wt%]	2.3	3.1	3.5
La_2O_3 [wt%]	2.5	3.4	3.8
MgO [wt%]	2.0	2.0	1.0
Si_3N_4 [wt%]	64.1	62.6	62.6
SiC [wt%]	28.0	27.4	27.4

formed by a reaction of sintering additives with SiO_2 from the surface of the Si_3N_4 powder particles. Since the liquid phase remains in the grain boundaries of the sintered ceramics it strongly influences the microstructural and mechanical properties. This intergranular phase was shown to play a critical role in the performance and lifetime of wood cutting tools, as shown in a previous studies.[7] Additives such as MgO, Al_2O_3, Y_2O_3 or mixtures thereof were found to be most effective in the earlier years of Si_3N_4 research.[11–13] MgO and Al_2O_3 are additives leading to a low viscous liquid which strongly promotes densification. Y_2O_3 forms a high viscous and refractory glass phase which increases the mechanical properties of Si_3N_4 ceramics.[14] Rare earth oxides, such as La_2O_3, Yb_2O_3 or Lu_2O_3, were investigated more recently. They increase the fracture toughness of Si_3N_4 ceramics by promoting the formation of elongated β-Si_3N_4 grains.[15–17]

There are several production methods for manufacturing dense Si_3N_4/SiC composites, e.g. hot pressing (HP),[12,18] pressure-less sintering (PLS)[18,19] or gas-pressure sintering (GPS).[20,21] The main advantage of HP is that complete densification can be achieved with a low amount of sintering additives due to the applied mechanical pressure. However, HP can produce only simple two-dimensional shapes. In PLS and GPS, which are more economical than HP, densification for low amounts of sintering additives is the main problem. Hot isostatic pressing can be performed on the presintered samples for further densification and enhancement of the mechanical properties.[19]

In the current work we developed Si_3N_4/SiC composites with varying composition of Al_2O_3, Y_2O_3, MgO and La_2O_3 sintering additives, for densification by PLS and GPS. The samples were HIPed and analysed for microstructure and mechanical properties. Then they were compared to samples prepared by HP having the same sintering additives. Density, hardness, fracture toughness, grain size and X-ray diffraction patterns were used for comparing the materials. Knives were manufactured from the most promising GPS composition. These were tested in a wood cutting trial and compared to HP knives. The goal was to develop a composition, suitable for industrial wood machining, which can easily be sintered.

2. Experimental details

Composites with varying amounts of sinter additives were prepared according to Table 1. The ratio of aluminium to lanthanum to yttrium atoms was kept constant, it was the same ratio as employed by Eblagon et al.[7] For composition A, 2 wt% MgO was added in order to enhance the densification of Eblagon's composition. The level of total additives was raised from 8 wt% for A to 10 wt% in compositions B and C. In composition C, the MgO content was reduced to 1 wt% for reducing the negative effect of MgO on the mechanical properties.[14]

The starting powders for the Si_3N_4/SiC composite were Si_3N_4 grade M11 and SiC grade UF25 (both H.C. Starck, Germany). The Si_3N_4 consists of 95% α-Si_3N_4 and of 5% β-Si_3N_4. MgO and La_2O_3 were added as $MgCO_3$ pentahydrate 99% (ABCR, Germany) and $La(OH)_3$ 99.9% (Auer Remy GmbH, Germany), respectively. The other sintering additives were Al_2O_3 (grade CT3000, Alcoa, Germany) and Y_2O_3 (grade C, H.C. Starck, Germany). The decompositions of $La(OH)_3$ and $MgCO_3$ were analysed by thermogravimetric analysis (TGA/SDTA851, Mettler Toledo, Switzerland). The specific surface areas were determined with the BET method (SA3100, Coulter Corporation, USA). The BET surface area of the starting powders Si_3N_4, SiC, $MgCO_3$, $La(OH)_3$, Al_2O_3 and Y_2O_3 were 12.7, 27.3, 10.0, 9.8, 7.2, 12.3 m^2/g. The sintering additives were ball milled in water for 2 h using Si_3N_4 balls with 5 mm diameter. Afterwards the Si_3N_4 and the SiC powder were added stepwise and the suspension was milled for another 48 h. 2 wt% polyethylene glycol (PEG 20000, Clariant GmbH, Germany) was added as a binder to the slurry after the milling process. Before granulation, the suspension was passed through a 64 μm sieve. The spray drying was performed on a Minor Hi-Tec apparatus (Niro S/A, Denmark). The particle size of the suspension and the dried granules were measured with a laser diffractometer (LS230, Beckman Coulter, Germany).

For HP, the granules filled into a BN coated graphite dye. The samples were hot pressed (Thermal Technology Co. USA) in nitrogen atmosphere. For PLS and GPS, the precursor powders were compacted uniaxially at 30 MPa and then cold isostatically pressed at 200 MPa. The binder was burnt out by heating the samples in air to 600 °C. The debinded green compacts were pressure-less sintered in a Si_3N_4/BN powder bed in a graphite furnace (FSW 315, KCE, Germany). The gas-pressure sintering of the green compacts was carried out in an industrial furnace (KCE, Germany). Finally, HP, GPS and PLS samples were all hot isostatically pressed (EPSI, Belgium) under nitrogen pressure. The sintering and HIP parameters including temperature, dwell time and pressure are summarised in Table 2.

The effective density of the sintered composites was determined by Archimedes principle. The relative theoretical density was calculated using the rule of mixtures. The Vickers hardness was determined following the procedure described in EN 843-4 using a weight of 2 kg.[22] The diagonals of the indents were measured with an optical microscope. Bend-bar specimens of 2 mm × 2.5 mm × 16 mm were cut out of the sintered composites by conventional diamond machining; the sides of the bend-bars were polished. However the edges of the samples were not chamfered. The strength values obtained by a three point bending test were thus used for comparative purposes of materials machined under identical conditions. The fracture toughness was determined on bend bars with a length of approximately 8 mm by a three point bending test of single-edge v-notched beams in accordance to Kübler.[23] The microstructure

Table 2
Sintering and heat treatment parameters for the processing of the Si_3N_4/SiC composites.

	Temperature [°C]	Dwell time [min]	N_2 pressure [MPa]	Mech. pressure [MPa]
Hot pressing	1800	30	0.1	35
Pressure-less sintering	1750	30	0.1	
Gas-pressure sintering	1860	30	7	
Post-hot isostatic pressing	1400	240	195	

of the polished and CF_4/O_2 plasma-etched samples were analysed by HR-SEM (Hitachi S-4800, Japan). The grain size of the β-Si_3N_4 grains was determined using the linear intercept method EN 623-3.[24] For each data point in density, bending strength, fracture toughness and grain size 5 samples were analysed. The grain boundary phase was analysed by transmission electron microscopy (TEM) (CM30, Philips). X-ray diffraction was carried out on polished samples using a PANanalytical XPert Pro diffractometer from Phillips, equipped with a Cu Kα radiation source to determine the types of crystalline phases present. The ratio of α- to β-Si_3N_4 was calculated according to the method developed by Gazzara et al.[25] The peaks from the (1 0 1) and the (3 0 1) planes were taken for α-Si_3N_4, peaks from the (1 1 0) and (2 0 0) planes for β-Si_3N_4. The wood cutting trials were performed on a moulding machine (GF Brugg Typ HAC, Switzerland) with automated feed. The feed rate was 12 m/min, the revolution speed 8000 min^{-1}, the tests were performed on spruce.

3. Results and discussion

3.1. Powder preparation

The sintering additive La_2O_3 was substituted by $La(OH)_3$, because La_2O_3 readily transforms into lanthanum hydroxide. In order to avoid coagulation of the slurry, MgO, which has an isoelectric point of 12.4,[26] was replaced by $MgCO_3$ having an IEP of about 9.[27] The pH of the slurry was adjusted to 11 using NH_3. At this pH the sintering additives, SiC and Si_3N_4 are negatively charged and form a stable suspension. The mean particle size of the slurry and the spray dried granules were 1.2 μm and 59.3 μm, respectively. The flowability of the spherical granules allowed an automated dye pressing into rectangular and circular green bodies. Thermogravimetric analysis of $La(OH)_3$ and $MgCO_3$ in air up to 1000 °C showed a mass loss of 14% and 57%. These mass losses were in accordance with the transformation from $La(OH)_3$ to La_2O_3 and $MgCO_3$ to MgO.

3.2. Sintering behaviour

Densification and elimination of the porosity has been shown to be a major step in the production of ceramic cutting tools with long lifetimes.[7] Fig. 1 gives the densities of the composites after the HP, GPS and PLS. The composites produced with PLS had the lowest relative densities in the range of 85–88%. The presence of more liquid phase leads to higher densities. PLS specimens with 10 wt% additives were therefore denser than the specimens with 7.9 wt% additives. MgO is a sintering additive which lowers the eutectic temperature and thus the viscosity of the liquid melt. Densification rates are therefore increased for MgO.[28] Hence, specimen B was denser than sample C. The above influences of total additive content and MgO level were not observed with the samples produced by pressure assisted sintering (GPS and HP). HIP could increase the density for PLS samples by about 5%. However, GPS and HP samples, which had already densities between 97.5% and 99%, did not densify a lot during HIP.

It is known that the density gain during HIP gets smaller as the starting densities of the samples approach theoretical densities. It is also known that the densification of silicon nitride ceramics by HIP is only possible if the presintered samples have densities above 94%, and thus open porosity had been eliminated. This was observed for example by Ziegler et al. who measured a decrease in density during HIP for samples with a starting density below 94%.[29] This finding is in contrast to the results obtained in this study. Ziegler et al. for example attributes the reduction of density to the evaporation of liquid phase during HIP at temperatures up to 1980 °C. The HIP temperature in the present study is 1400 °C. Therefore, an evaporation of the liquid phase is unlikely and an increase in density during HIP might thus be possible. Nevertheless, the densities of PLS composites produced in this study were too low for the application as a wood cutting tool, and these samples were not further investigated. Greil et al. showed that the fabrication of dense Si_3N_4/SiC composites by PLS and HIP is possible by the addition of 15 wt% additives.[19] However, an increase in the concentration of additives is known to reduce the mechanical properties, especially at elevated temperature.[28]

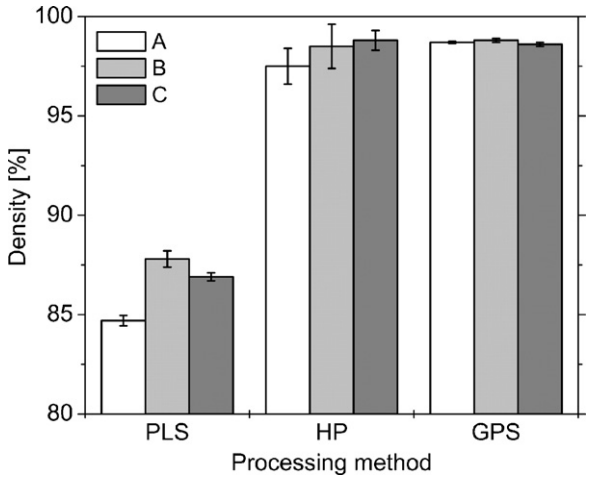

Fig. 1. Measured densities (compared to theoretical density) of samples sintered with different processing methods. Composition A contained 7.9 wt% sintering aids, while B and C had 10 wt% additives.

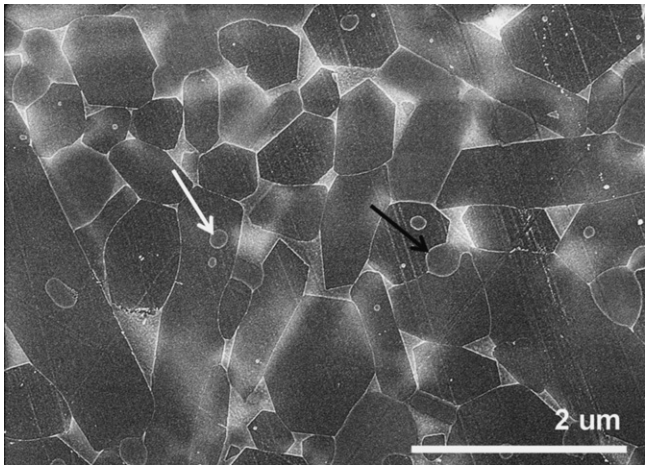

Fig. 2. HR-SEM images of the GPS/HIP sample of composition A. The hexagonal β-Si_3N_4 grains were etched, while SiC and intergranular phase remained unattacked. SiC grains can be found in intragranular (white arrow) and intergranular (black arrow) position.

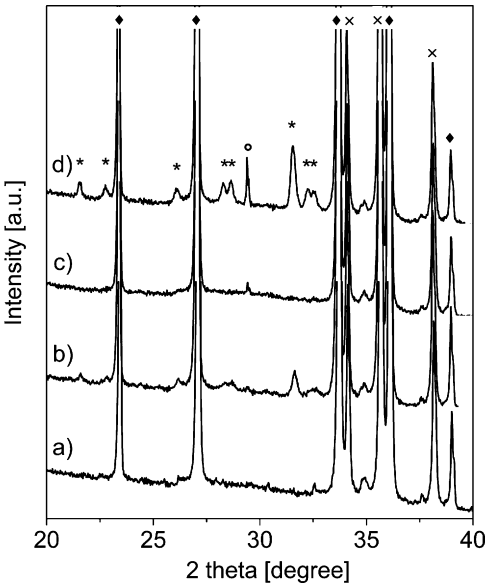

Fig. 3. XRD patterns of GPS specimen A without HIP cycle (a), A GPS/HIP (b), B GPS/HIP (c) and C GPS/HIP (d). (♦) β-Si_3N_4; (×) SiC; (◯) $Y_2Si_2O_3$; (*) $Y_5Si_3O_{12}N$.

3.3. Microstructural characterisation

Fig. 2 shows a SEM micrograph of the GPS sample A. The sample was treated in CF_4/O_2 plasma. This leads to a favoured etching of the Si_3N_4 grains, while SiC grains and the intergranular phase undergo insignificant, if any, attack.[30] The β-Si_3N_4 grains were visible as dark grey hexagonal areas. They occupy $65 \pm 3\%$ of the area of the micrograph, as was calculated by image analysis. This was in good agreement with the addition of 64 wt% Si_3N_4 in the starting powder. SiC could be found in inter- and intragranular position. The ternary phase, containing the sintering additives, was identified as a light film around the β-Si_3N_4 grains and in the multiple grain junctions. XRD patterns of GPS/HIP and HP/HIP specimens reveal that the phase transformation from α-Si_3N_4 to β-Si_3N_4 was completed in the GPS samples. However 5 wt% α-Si_3N_4 remained in the HP specimens. This might be due to the shorter processing time, which allows less time for the phase transformation. The XRD patterns showed that the intergranular phase had a glassy character after sintering for both HP and GPS samples. The intergranular phase devitrified during the HIP treatment. As an example, Fig. 3 gives the XRD spectra for GPS samples before and after HIP. In the GPS sample with composition A, the H-phase $Y_5Si_3O_{12}N$ was identified. In composition B the phase $Y_2Si_2O_7$ was present, while sample C contained both the H-phase and $Y_2Si_2O_7$-phase. The H-phase was also the predominant phase in the samples prepared by hot pressing. TEM and selected area diffraction analysis confirmed the crystalline nature of the intergranular phase in HP/HIP samples, see Fig. 4. Rendtel et al. annealed Si_3N_4/SiC composites with 12 wt% Y_2O_3 at 1400 °C for 24 h. The H-phase, as well as the M- and K-phase ($Y_2Si_3N_4O_3$ and $YNSiO_2$, respectively) were identified in their samples.[20] They stated that the above crystallisation treatment increases the creep resistance of the GPS composite.

The grain sizes of the HP/HIP and GPS/HIP samples, determined with the linear intercept method, are given in Fig. 5. The finer grains in the HP/HIP samples might evolve due to the external mechanical pressure during sintering which increases the nucleation rate.[28] Another reason could be the shorter processing time in HP, which allows less time for grain growth. For the production of a sharp cutting tip, with radius <2 μm, it is important to have a grain size <0.5 μm. The variation of the average grain size for one processing method was within the standard deviation of the measurement.

3.4. Mechanical properties

Fig. 5 gives the Vickers hardness of the HP/HIP and the GPS/HIP specimen. The hardness was higher for the HP/HIP

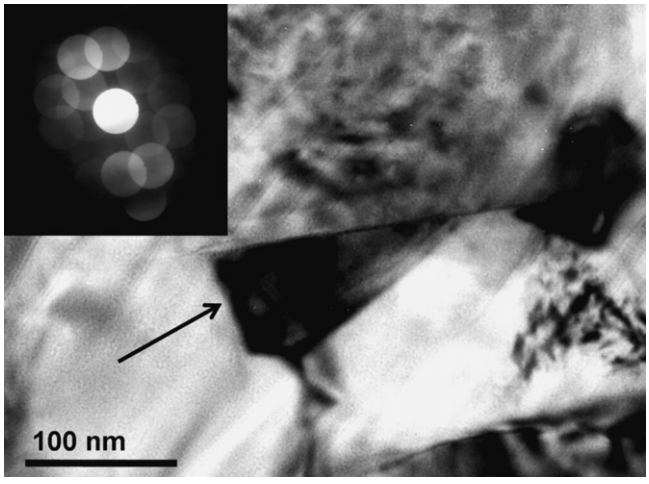

Fig. 4. TEM pictures of HP/HIP specimen, including SAD pattern of the intergranular crystallised phase (arrow), which is surrounded by hexagonal β-Si_3N_4 grains.

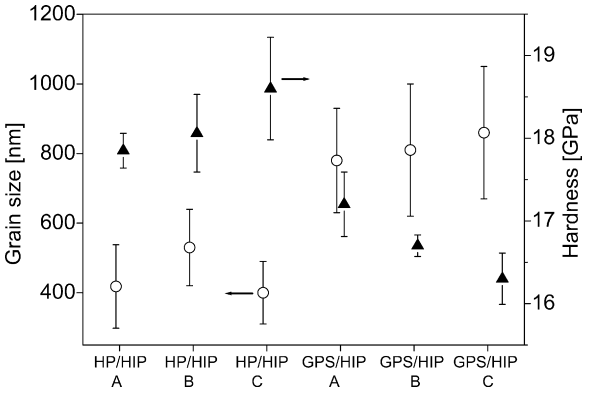

Fig. 5. Average grain size of β-Si_3N_4 grains and Vickers hardness of GPS/HIP and HP/HIP samples having different compositions.

samples than for the GPS/HIP sample. Rice et al. stated that the hardness typically increases with decreasing grain size in the finer grain size region.[31] The HP/HIP specimens had finer grains than the GPS/HIP samples and therefore showed higher hardness. The best value for GPS samples was 17.2 ± 0.4 GPa for composition A. The hardness of the composite produced by Eblagon et al. via hot pressing was 19 GPa.[7] The reason for the lower hardness in this study might be the use of more sintering additives and the addition of MgO. Nevertheless, the addition of MgO was necessary in order to optimise composite and reach 99% density by GPS. A high hardness is better for the wear properties of a cutting tool, but on the other hand, a high hardness hampers the machinability of the knife edge. Good machinability is important on one side for the quality of the cutting edge, and on the other side for reducing the production costs. The fracture toughness of the HP/HIP and GPS/HIP specimens is reported in Fig. 6. Shaoming reported a fracture toughness of 5.4 MPa$\sqrt{}$m for a CMC with 6 wt% La_2O_3 and Y_2O_3 additives, fabricated by encapsulated HIP.[32] The fracture toughness of the samples produced in this research is in the range of 4.5 MPa$\sqrt{}$m for all compositions, independent of the production process. The bending strength is shown in Fig. 6. In GPS samples with larger grains, the bending strength was higher than in the equivalent HP samples. A decrease in grain size normally causes an increase in

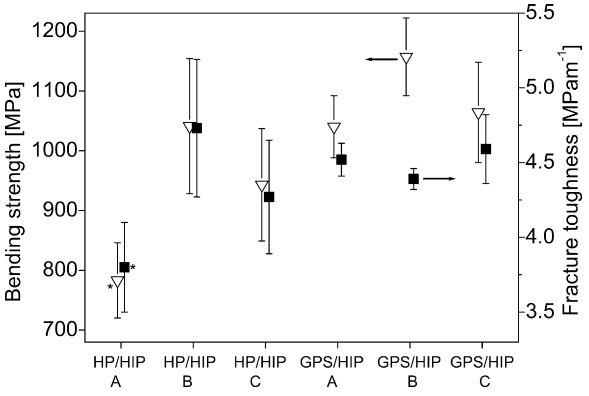

Fig. 6. Three point bending strength (samples without chamfer) and fracture toughness (SEVNB-method) of samples produced by HP/HIP and GPS/HIP, having different compositions. *The powder for this composition was made by evaporation and grinding and not by spray drying.

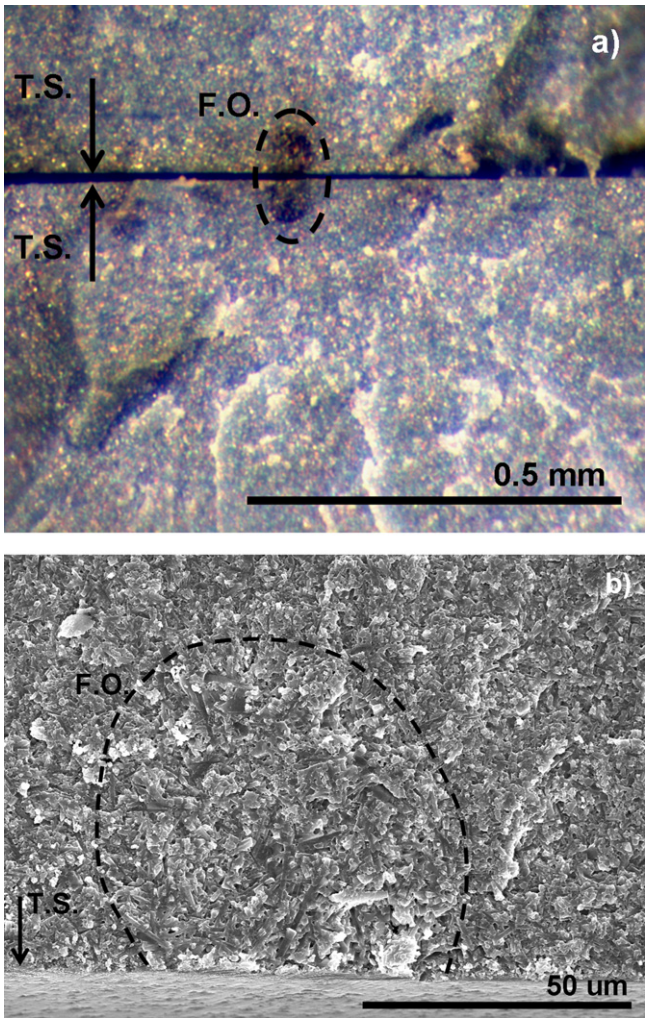

Fig. 7. Pictures of the origin of fracture of GPS/HIP bend bar composition C with a bending strength of 1024 MPa. (a) Optical microscopy image of the two fracture pieces. (b) SEM image of the origin of fracture. T.S. tensile surface, F.O. fracture origin.

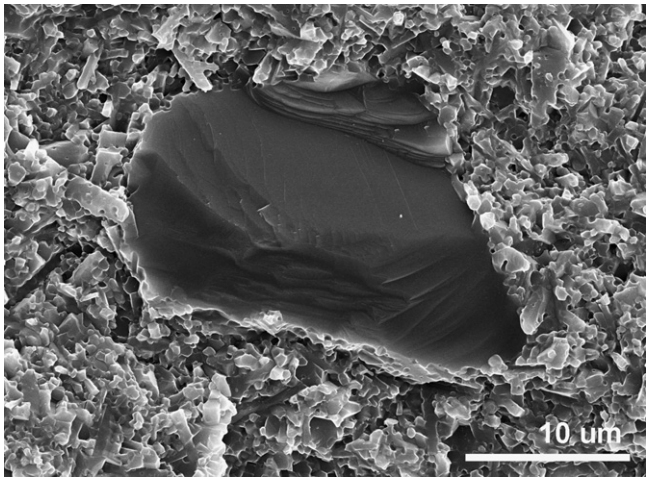

Fig. 8. SEM picture of a dense silicon rich cluster, found on the fracture surface of the GPS/HIP bend bars.

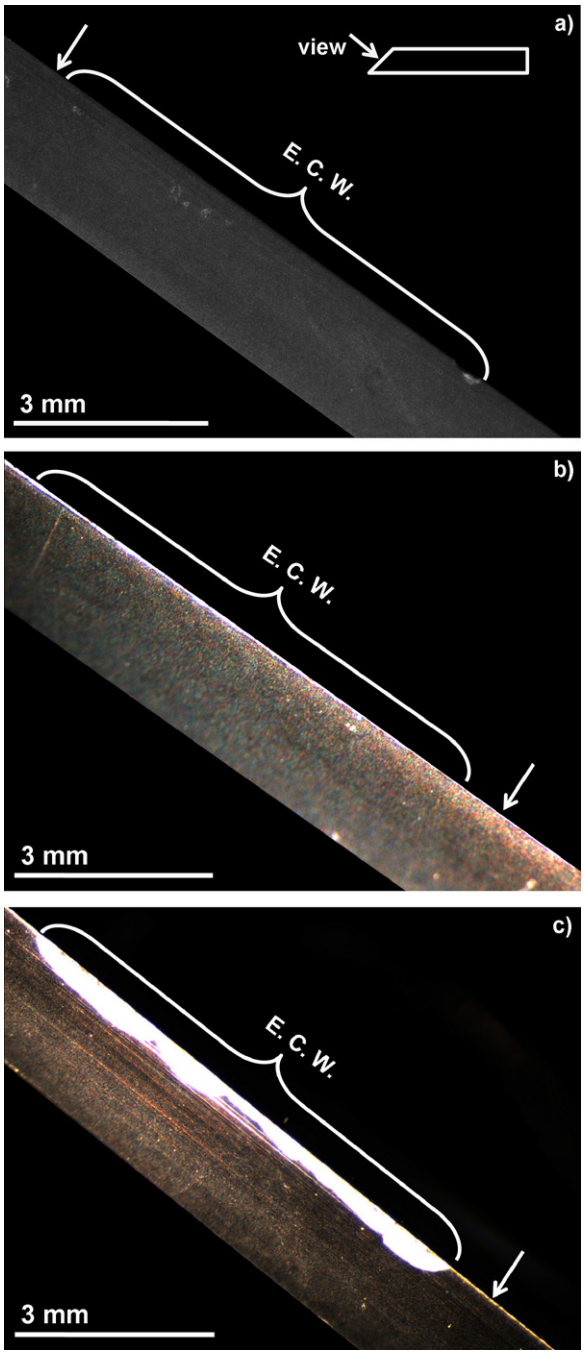

Fig. 9. Optical microscopy pictures of the cutting edge (arrow) of samples after the cutting trial on wood. Sketch shows the viewing angle of the images. (a) Knife made by GPS/HIP of composition A, knives produced by HP/HIP (b) and HP (c). E. C. W. edge in contact with wood.

bending strength.[33] There must be other influences, such as the anisotropy of HP samples, or the differences in aspect ratio of the β-Si_3N_4 grains, which could increase the strength in GPS samples. A comparison of bending strength values with the literature was omitted, as the tested bend bars had smaller dimensions than standard bars and no chamfered edges. There was no measurable effect of the type of intergranular phases on the hardness, bending strength and fracture toughness. Fractography by optical microscopy and SEM were performed on the bend bars. Optical microscopy revealed that black spots were the origins of fracture in GPS/HIP and HP/HIP bend bars (see Fig. 7). SEM revealed that these black spots were made up of more and longer β-Si_3N_4 grains than the surrounding area, some porosity was found too. EDX showed that the area of the fracture origin was enriched in sintering additives. This accumulation of sintering additives led to an increased grain growth and a more elongated morphology of β-Si_3N_4 grains. An optimisation of the processing, e.g. the ball milling, could avoid such inhomogeneities in the composites. There was a second type of defect found on the fracture surface, which were dense agglomerates, see SEM picture in Fig. 8. These clusters were found on GPS/HIP samples only. The shear bands on the agglomerates were an indication for the crystalline nature of these clusters. Semi-quantitative EDX showed that the cluster compared to the matrix was silicon rich, but depleted in sintering additives, oxygen and nitrogen. This suggests that the clusters could be agglomerates of SiC, which formed during the sintering process by decomposition of Si_3N_4.

3.5. Cutting trials

Based on the microstructural and mechanical properties, especially the hardness, composition A was chosen to be the most suitable among the GPS specimens for the wood cutting trials. In Fig. 9a and b the cutting edge of knife GPS/HIP A was compared to knives prepared by HP/HIP. The GPS/HIP knives nearly show the same performance as HP/HIP knives. However, some minor chips are visible. A reason for this could be the already discussed agglomerates which were found during the fractographic analysis, or the lower hardness compared to HP/HIP specimens. Furthermore, Fig. 9c shows that the post-HIP treatment is indispensable for the integrity of the cutting edge. This increase in cutting tip integrity was due to the crystallisation of the grain boundary triple points as shown by XRD and TEM. And due to the crack healing behaviour of Si_3N_4/SiC ceramics during HIP, which can reduce the defect size introduced by diamond machining.[34]

4. Conclusion

This study showed that gas-pressure sintering is a suitable near net-shape process for the production of dense Si_3N_4/SiC composites for the use as wood cutting inserts.

- Compared to hot pressed composites, gas-pressure sintered samples display higher bending strength, lower hardness and larger grain size.
- GPS/HIP knives almost reach the performance of HP/HIP knives in the cutting trial on wood.
- Hot isostatic pressing after machining of the cutting inserts is indispensable for good cutting edge integrity. This is due to the crystallisation of the intergranular phase into $Y_2Si_2O_7$ and/or $Y_5Si_3O_{12}N$ as was proven by XRD and TEM analysis.
- Gas-pressure sintering produced composites with 98.5–99% relative densities. This is similar to what was obtained by hot pressing. However the processing has to be optimised in

order to eliminate the clusters of SiC and the inhomogeneous distribution of sintering additives.
- PLS of Si_3N_4/SiC composites produced densities of less than 93%, this is insufficient for a good cutting tool.

Future work will include optimisation of the processing and further cutting trials with GPS/HIP knives. Additionally, the authors will investigate the evolution of the intergranular crystalline phases as a function of the HIP parameters and its influence on the cutting performance.

Acknowledgements

The authors would like to thank F. Alvarez, for his assistance with diamond machining of the bend bars, R. Bächtold for help with the mechanical tests and H. Hank and M. Hellstern from Ceratizit Horb GmbH for diamond machining of the cutting inserts. We thank Dr. M. Parlinska for the help with the TEM study and Prof. C. Aneziris from the Technical University of Freiberg for the helpful discussions. Part of this work was supported by the Swiss Commission for Technology (CTI) under the contract number 8989.1PFIW-IW.

References

1. Stewart HA. High temperatures wear tools when wood machining. *Mod Woodworking* 1993:1–4.
2. Costes J-P, Larricq P. Towards high cutting speed in wood milling. *Ann Forest Sci* 2002;**59**:857–65.
3. Pugsley VA, Korn G, Luyckx S, Sockela HG, Heinrich W, Wolf M, et al. The influence of a corrosive wood-cutting environment on the mechanical properties of hardmetal tools. *Int J Refr Met Hard Mater* 2001;**19**:311–8.
4. Sheikh-Ahmad JY, Bailey JA. The wear characteristics of some cemented tungsten carbides in machining particleboard. *Wear* 1999;**225–229**:256–66.
5. Gauvent M, Rocca E, Meausoone PJ, Brenot P. Corrosion of materials used as cutting tools of wood. *Wear* 2006;**261**:1051–5.
6. Matienssen W, Warlimont H. *Springer handbook of condensed matter and materials data*. Berlin, Heidelberg: Springer; 2005. p. 451–72.
7. Eblagon F, Ehrle B, Graule T, Kuebler J. Development of silicon nitride/silicon carbide composites for wood-cutting tools. *J Eur Ceram Soc* 2007;**27**:419–28.
8. Djouadi MA, Beer P, Marchal R, Sokolowska A, Lambertin M, Precht W, et al. Antiabrasive coatings: application for wood processing. *Surf Coat Technol* 1999;**116–119**:508–16.
9. Faga MG, Settineri L. Innovative anti-wear coatings on cutting tools for wood machining. *Surf Coat Technol* 2006;**201**:3002–7.
10. Gogolewski P, Klimke J, Krell A, Beer P. Al_2O_3 tools towards effective machining of wood-based materials. *J Mater Proc Technol* 2009;**209**:2231–6.
11. Terwilliger GR, Lange FF. Hot-pressing behaviour of Si_3N_4. *J Am Ceram Soc* 1974;**57**:25–9.
12. Hirano T, Niihara K. Microstructure and mechanical properties of Si_3N_4/SiC composites. *Mater Lett* 1995;**22**:249–54.
13. Tanaka H, Greil P, Petzow G. Sintering and strength of silicon nitride–silicon carbide composites. *Int J High Tech Ceram* 1985;**1**:107–18.
14. Petzow G, Herrmann M. *Silicon nitride ceramics. Structure and bonding*. Berlin: Springer; 2002. p. 50–167.
15. Satet RL, Hoffmann MJ, Cannon RM. Experimental evidence of the impact of rare-earth elements on particle growth and mechanical behaviour of silicon nitride. *Mater Sci Eng: A* 2006;**422**:66–76.
16. Hoffmann MJ. Analysis of microstructural development and mechanical properties of Si_3N_4 ceramics. In: Hoffmann MJ, Petzow G, editors. *Tailoring of mechanical properties of Si_3N_4 ceramics*. Netherlands: Kluwer Academic Publishers; 1994. p. 59–72.
17. Satet RL, Hoffmann MJ. Influence of the rare-earth element on the mechanical properties of RE_2O_3; Mg-bearing silicon nitride. *J Am Ceram Soc* 2005;**88**:2485–90.
18. Biasini V, Guicciardi S, Bellosi A. Silicon nitride–silicon carbide composite materials. *Int J Refr Met Hard Mater* 1992;**11**:213–21.
19. Greil P, Petzow G, Tanaka H. Sintering and HIPping of silicon nitride–silicon carbide composite materials. *Ceram Int* 1987;**13**:19–25.
20. Rendtel P, Rendtel A, Hubner H. Mechanical properties of gas pressure sintered Si_3N_4/SiC nanocomposites. *J Eur Ceram Soc* 2002;**22**:2061–70.
21. Herrmann M, Schuber C, Rendtel A, Hubner H. Silicon nitride/silicon carbide nanocomposite materials. I. Fabrication and mechanical properties at room temperature. *J Am Ceram Soc* 1998;**81**:1095–108.
22. EN 843-4. Advanced Technical Ceramics – Monolithic Ceramics – Mechanical Properties at Room Temperature. Part 4. Vickers, Knoop and Rockwell Superficial Hardness Tests.
23. Kübler J. Fracture toughness of ceramics using the SEVNB method: from a preliminary study to a standard test method, fracture resistance testing of monolithic and composite brittle materials. In: Salem JA, Jenkins MG, Quinn GD, editors. *ASTM STP 1409*. West Conshokocken: ASTM; 2002. p. 93–106.
24. EN 623-3. Advanced Technical Ceramics – Monolithic Ceramics – General and Textural Properties. Part 3. Determination of Grain Size and Size Distribution (Characterized by the Linear Intercept Method).
25. Gazzara CP, Messier DR. Determination of phase content of Si_3N_4 by X-ray diffraction analysis. *Ceram Bull* 1977;**56**:777–80.
26. Kosmulski M. The pH-dependent surface charging and the points of zero charge. *Colloid Interface Sci* 2002;**253**:77–87.
27. Skvarla J, Kmet S. Non-equilibrium electrokinetic properties of magnesite and dolomite determined by the laser-Doppler electrophoretic light scattering (ELS) technique. A solids concentration effect. *Colloid Surf A: Physicochem Eng Aspects* 1996;**111**:153–7.
28. Ziegler G, Heinrich J, Wötting G. Review: relationship between processing, microstructure and properties of dense and reaction-bonded silicon nitride. *Mater Sci* 1987;**22**:3041–86.
29. Ziegler G, Wotting G. Post-treatment of pre-sintered silicon nitride by hot isostatic pressing. *Int J High Tech Ceram* 1985;**1**:31–58.
30. Pink FX, Ostreicher KJ. Transmission electron microscopy studies of plasma-etched silicon nitride/silicon carbide composites. *Electron Microsc Tech* 1987;**7**:161–6.
31. Rice RW, Wu CC, Fred B. Hardness-grain-size relations in ceramics. *J Am Ceram Soc* 1994;**77**:2539–53.
32. Shaoming D, Jiang D, Tan S, Guo J. Hot isostatic pressing of SiC/Si_3N_4 composite with rare earth oxide additions. *Ceram Int* 1995;**21**:451–5.
33. Rice R. Ceramic tensile strength-grain size relations: grain sizes, slopes, and branch intersections. *Mater Sci* 1997;**32**:1673–92.
34. Jung Y-S, Nakao W, Takahashi K, Ando K, Saito S. Crack healing of machining cracks introduced by wheel grinding and resultant high-temperature mechanical properties in a Si_3N_4/SiC composite. *J Am Ceram Soc* 2009;**92**:167–73.